Self-Heating in GaN Transistors Designed for High-Power Operation

Ján Kuzmík, Milan Ťapajna, Lukas Válik, Marian Molnár, Daniel Donoval, Clément Fleury, Dionyz Pogany, Gottfried Strasser, Oliver Hilt, Frank Brunner, and Joachim Würfl

***Abstract*— DC and transient self-heating effects are investigated in normally off AlGaN/GaN transistors designed for a high-power operation. Electrical and optical methods are combined with thermal simulations; 2-μs-long voltage pulses dissipating about 4.5 W/mm are applied on four different transistor structures combining GaN or AlGaN buffer on an n-type SiC substrate with or without Ar implantation. Transistors with only 5% Al mass fraction in the buffer show almost a threefold increase in the transient self-heating if compared with devices on the GaN buffer. On the other hand, 2-μs-long pulses were found not to be long enough for the Ar-implanted SiC substrate to influence the device self-heating unless AlGaN composition changes. In the dc mode, however, both the buffer composition and Ar implantation significantly influence the self-heating effect with the highest temperature rise for the transistor having the AlGaN buffer grown on the Ar-implanted SiC. We point on possible tradeoffs between the transistor high-power design and the device thermal resistance.**

***Index Terms*— GaN, high-electron mobility transistor (HEMT), optical characterization, thermal characterization, thermal resistance.**

I. Introduction

GaN-BASED transistors are considered to be excellent candidates for high-power and efficient switching applications [1]. Various design issues were investigated in the past to boost the device performance. The usage of a Fe-doped GaN or AlGaN buffer instead of an ordinary undoped GaN was suggested to increase the device breakdown voltage while maintaining a low dynamical on-resistance [2]. Similarly, Ar implantation in the n-type SiC substrate was shown to improve a vertical blocking voltage in GaN high-electron mobility transistor (HEMT) [3], [4]. However, no attention was particularly given to investigate an impact of the mentioned or similar design changes on the device self-heating. Elevated temperature during the operation of GaN-based transistor may deteriorate the device performance [5] and reliability [6]. In this paper, we investigate dc and transient self-heating effects in tailored designed high-power normally off GaN HEMTs using electrical [7], [8] and optical [9] methods.

Manuscript received June 13, 2013; revised August 6, 2014; accepted August 18, 2014. Date of publication September 8, 2014; date of current version September 18, 2014. This work was supported in part by the European Union FP7 HipoSwitch Project under Grant 287602, in part by the Slovak Project under Grant DO7RP-0021-11, and in part by the VEGA Project under Grant 0866/11. The review of this paper was arranged by Editor R. Venkatasubramanian.

J. Kuzmík, M. Ťapajna, and L. Válik are with the Institute of Electrical Engineering, Slovak Academy of Sciences, Bratislava 841 04, Slovakia (e-mail: jan.kuzmik@savba.sk; milan.tapajna@savba.sk; lukassvalik@gmail.com).

M. Molnár, D. Donoval are with Institute of Electronics and Photonics, Slovak University of Technology, Bratislava, Slovakia. (e-mail: xmolnarm1@gmail.com; daniel.donoval@stuba.sk).

C. Fleury, D. Pogany, and G. Strasser are with the Institute for Solid State Electronics, Vienna University of Technology, Vienna 1040, Austria (e-mail: clement.fleury@tuwien.ac.at; dionyz.pogany@tuwien.ac.at; gottfried.strasser@tuwien.ac.at).

O. Hilt, F. Brunner, and J. Würfl are with Ferdinand-Braun-Institut, Leibniz Institut für Höchstfrequenztechnik, Berlin 12489, Germany (e-mail: oliver.hilt@fbh-berlin.de; frank.brunner@fbh-berlin.de; hans-joachim.wuerfl@fbh-berlin.de).

Color versions of one or more of the figures in this paper are available online at http://ieeexplore.ieee.org.

Digital Object Identifier 10.1109/TED.2014.2350516

II. Devices and Methods

Investigated AlGaN/GaN/AlGaN HEMT devices use a p-type gate technology [10]. All devices were metal-organic chemical vapor deposition grown on the n-type SiC, with or without Ar implantation. The epi-structures comprise AlN seeding layer, AlGaN buffer with targeted 5% Al mass fraction or alternatively a sequence of Fe-doped and undoped GaN, AlGaN barrier layer, and p-type GaN (Table I). Combinations of different buffers and/or implantation define structures A–D. Structures were depleted from electrons due to p-GaN. As reported elsewhere, after removing p-GaN layer, Hall-measurement data indicated about 10% drop in electron concentration data in heterostructures with AlGaN buffer if compared with GaN ones, from 7.27×10^{12} down to 6.58×10^{12} cm^{-2}, with only minor change in mobility from 1615 down to 1535 cm^2/Vs [4]. With Ar implantation, changes were between -1% and -5% [4]. Lateral device geometrical dimensions were gate length $L_G = 1.3$ μm, gate width $w = 2 \times 1.05$ mm, gate-to-drain distance $d_{GD} = 15$ μm, and source-to-gate distance $d_{SG} = 1$ μm. Wafers were diced to chips with a size of 1.8 mm $\times$ 3.76 mm $\times$ 0.36 mm and brazed on copper flanges. Other technological details can be found elsewhere [2], [3], [10].

Self-heating was monitored in the steady state and during 2-μs-long voltage pulses (1.8 μs after subtracting the rising edge). The dc steady-state method is based on the effect of the HEMT saturated drain current drop $\Delta I_{sat}(V_D)$ as the drain voltage is increased. This effect was described analytically as [7]

$$\Delta I_{sat}(V_D) = -g_m(I_{sat}\Delta R_S + \Delta V_T) + I_{sat}\Delta v_{sat}/v_{sat} + V_D/R_{out} \quad (1)$$

TABLE I
EPI-STRUCTURE DETAILS OF STUDIED STRUCTURES. CHANNEL THICKNESS IS INDICATED ONLY FOR AlGaN BUFFER SAMPLES A AND B

Structure	SiC substrate	AlN thickness	Buffer type	Buffer thickness	Channel thickness	AlGaN barrier	p-GaN
A	n-type	100 nm	AlGaN	3560 nm	35 nm	14 nm 24 %	103 nm
B	n-type + Ar	100 nm	AlGaN	3560 nm	35 nm	14 nm 24 %	103 nm
C	n-type	80 nm	200 nm nidGaN + 2070 GaN:Fe + 880 nm nidGaN			14 nm 23 %	102 nm
D	n-type + Ar	80 nm	200 nm nidGaN + 2070 GaN:Fe + 880 nm nidGaN			14 nm 23 %	102 nm

where g_m is the transconductance, ΔR_S, ΔV_T, and $\Delta v_{\rm sat}$ are temperature-driven changes in a source resistance, threshold voltage and electron saturation velocity, respectively. V_D represents the drain voltage, and $R_{\rm out}$ represents a differential output resistance. Calibrating steady-state dependencies of the transistor parameters on temperature (ΔR_S and $\Delta V_T = f(T)$, $\Delta v_{\rm sat}$ is neglected introducing about 10% overestimation in T), it is possible to determine the HEMT channel temperature as a function of dissipated power $V_D x I_{\rm sat}$.

To describe a temperature-induced *time-dependent* current drop $\Delta I_{\rm sat}(t)$, we use methodology of the dc method, considering several differences [8]. First of all, as the voltage is kept constant during pulses, the same is assumed for the buffer/drain modulation leakage current and the last term in (1) could be neglected. Similarly, for a relatively short duration of the pulse, we neglected trap-related ΔV_T. Therefore, $\Delta I_{\rm sat}(t)$ can be expressed as

$$\Delta I_{\rm sat}(t) = -g_m I_{\rm sat} \Delta R_S. \tag{2}$$

Using a polynomial fit to calibration curves $\Delta R_S = f(T)$, and $g_m(T) = g_m(300\ \text{K})/[1+g_m(300\ \text{K}) \times \Delta R_S(T)]$ together with the measured $\Delta I_{\rm sat}(t)$, an iterative solution of (2) could be performed to obtain the channel temperature transient characteristics [8].

To determine ΔR_S at different T, initially, we determine $R_{S,D} = R_S + R_D$ by extrapolating a total source-to-drain resistance R_T dependence to $V_x = 1/\{1 - [(\Phi_b - V_{\rm GS})/(\Phi_b - V_T)]\} = 0$ V [11], where $\Phi_b \sim 3.8$ V is given by a p-n junction built-in voltage and conduction band discontinuity at p-GaN/AlGaN interface. Then, R_S is calculated as $(R_{S,D} - 2 \times R_C) \times d_{\rm SG}/(d_{\rm SG} + d_{\rm GD}) + R_C$, where $R_C = 0.2\ \Omega$mm is the contact resistance.

In the transient interferometric mapping (TIM) method, the device is scanned from the backside using an infrared laser beam (3 ns, 1.5-μm resolution). A phase shift $\Delta\varphi$ of a reflected beam (from the topside) is caused by a temperature-induced change in a material refractive index n along the beam path L and can be expressed as [12]

$$\Delta\varphi(x, y, t) = \frac{4\pi}{\lambda} \int_0^L \frac{dn}{dT} \Delta T(x, y, z, t) dz. \tag{3}$$

Here, λ is a laser wavelength and x and y are lateral coordinates. The TIM method operates in the transient (pulsed) regime of the self-heated device and can be used to trace the lateral and vertical spreading of the heat [8], [9].

To simulate and explain self-heating effects in the transient state of the devices, we used a 2-D thermal model SDevice from Synopsys [13]. We used thermal conductivity values (at room temperature) $K_{\rm GaN} = 150$ W/mK [14] and $K_{\rm SiC} = 490$ W/mK [9], while $K_{\rm AlGaN}$ of the buffer layer was used as a fitting parameter. Substantial drop in $K_{\rm AlGaN}$ even for a low Al mass fraction in the buffer can be expected [14]. Similarly, decreased $K_{\rm SiC}$ can be expected in the top 300 nm of the implanted substrate where Ar penetrates [3]. Effective $K_{\rm AlN} = 2$ W/mK was chosen to simulate a thermal boundary resistance at the substrate/nitride interface to be 5×10^{-8} m^{2}K/W [9], [15]. Both $K_{\rm GaN}$ and $K_{\rm AlGaN}$ are assumed to be temperature dependent [14] with a factor T^{-1}.

III. RESULTS AND DISCUSSION

A. Device Calibration

Fig. 1(a)–(d) shows dc characteristics of the studied GaN-based normally off transistors. Slightly lower $I_{\rm sat}$ were observed for AlGaN buffer structures A and B, because of a depletion effect introduced by the back-barrier [11]. Note the pronounced negative differential output conductance in all studied transistors, particularly for structures A and B starting already at $I_{\rm sat} \sim 100$ mA/mm. This phenomenon indicates unusually strong self-heating effects even though SiC has been used as a substrate. Large total gate width combined with small chip dimensions and a limited heat removal to the flange can account for this effect. Thermal calibrations of R_S (starting from $\sim$1 Ωmm at room temperature) up to 180 °C are documented in Fig. 2 as ΔR_S, including polynomial fits to the experimental data. Similarly, V_T dependences were fitted to describe the observed V_T rise between 150 mV for structure D and 500 mV for structure A, respectively (not shown). Fig. 3 shows the current and voltage waveforms during 2-μs-long voltage pulses applied on each transistor at different gate bias points to dissipate about 4.5 W/mm in average. About 200-ns-long rising edges including short RC-related humps were neglected by temperature extractions.

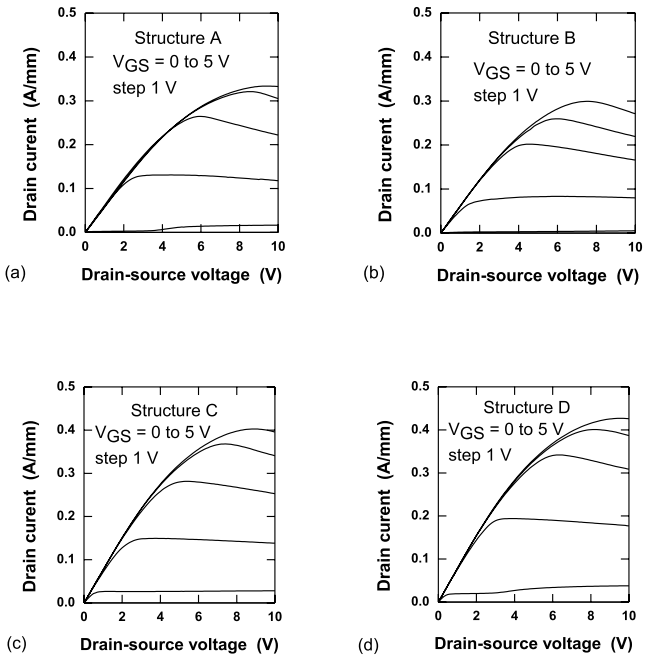

Fig. 1. DC output characteristics of structure (a) A, (b) B, (c) C and (d) D.

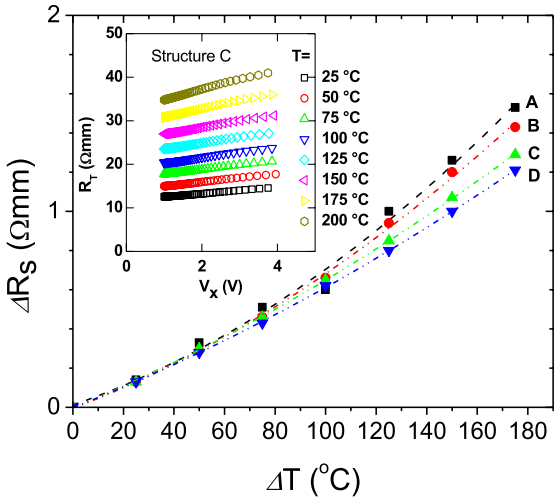

Fig. 2. Thermal calibration of the source resistance R_S of structures A–D. Inset shows source-to-drain resistance R_T of structure C measured at $V_D = 100$ mV at different T as a function of $V_x = 1/\{1 - [(\Phi_b - V_{GS})/(\Phi_b - V_T)]\}$.

B. Transient Self-Heating

Extracted T transients, including simulation curves, are shown in Fig. 4. Almost identical and the lowest self-heating effects were observed for structures C and D, while the effect becomes dramatically stronger for structures A and B. Best fits were observed with $K_{\mathrm{AlGaN}} = 30$ W/mK for structure A and $K_{\mathrm{AlGaN}} = 15$ W/mK for structure B. On the other hand, simulated transient self-heating effects were found to be practically invariant to the thermal conductivity value of Ar-implanted SiC for all structures (not shown). This analysis suggest that: 1) transient self-heating effect is dramatically increased by replacing GaN buffer with AlGaN and 2) 2-μs-long pulse is short enough to prevent a significant heat penetration to the substrate. Later finding is supported

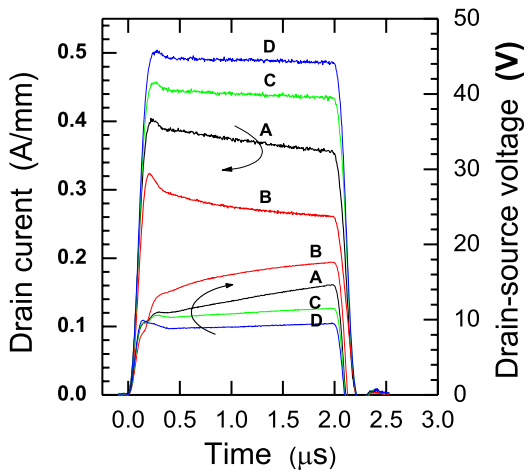

Fig. 3. Current–voltage waveforms of structures A–D during 2-μs-long pulses dissipating about 4.5 W/mm.

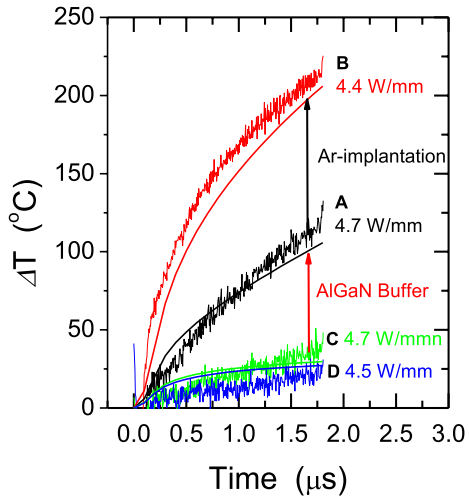

Fig. 4. Extracted (noisy lines) and calculated (full lines) temperature rises in structures A–D. In calculations, time evolutions of dissipated power levels are taken from waveforms shown in Fig. 3, and the average dissipated power values are marked close to each line. Arrows highlight the changes introduced to self-heating by different technological designs.

also by calculated T depth profiles at the end of pulses where negligible T rises in SiC can be inferred from Fig. 5. Thus, the most pronounced self-heating effect observed in Ar-implanted structure B can be related to lower K_{AlGaN} compared with that of structure A rather than to modified K_{SiC}. We note that the AlGaN buffer is slightly thicker than the GaN buffer. Nevertheless, qualitative differences in self-heating between GaN and AlGaN buffer devices shown in Fig. 5 would be even more pronounced having the same buffer thicknesses because of the heat confinement imposed by the thermal boundary resistance at the buffer/SiC interface.

Our findings were further supported by TIM experiments showing similar signal evolutions for structures C and D, while there are clear differences between the phase shifts for structures A and B (Fig. 6). Moreover, TIM signals for structures A and B with AlGaN buffer are overall reduced if compared with structures C and D, with the lowest signal for structure B. This is because the thermo-optical parameter *dn/dT* of AlGaN is supposed to be lower than that of GaN [16].

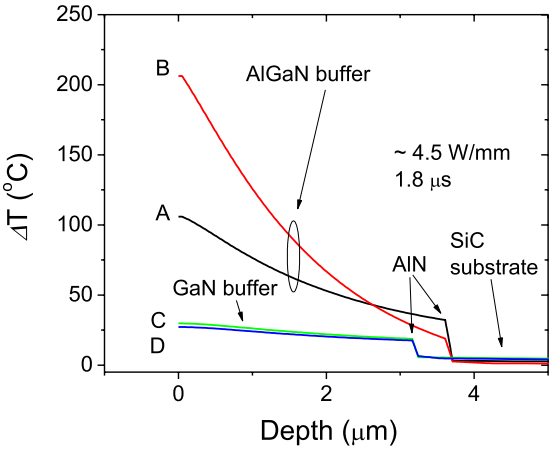

Fig. 5. Calculated temperature rises in the cross section of the devices at the end of 1.8-μs-long pulses dissipating about 4.5 W/mm.

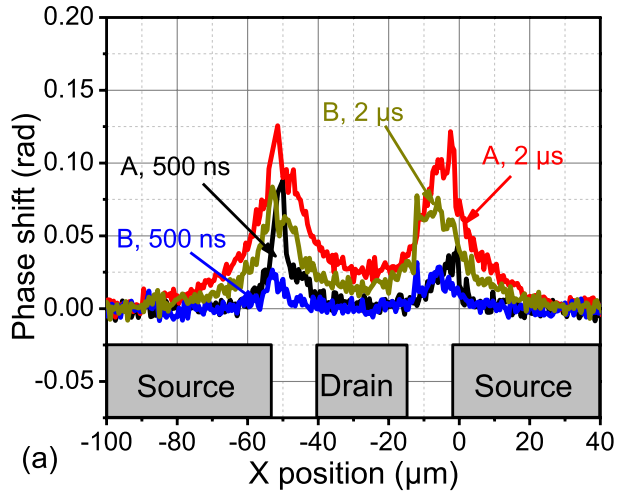

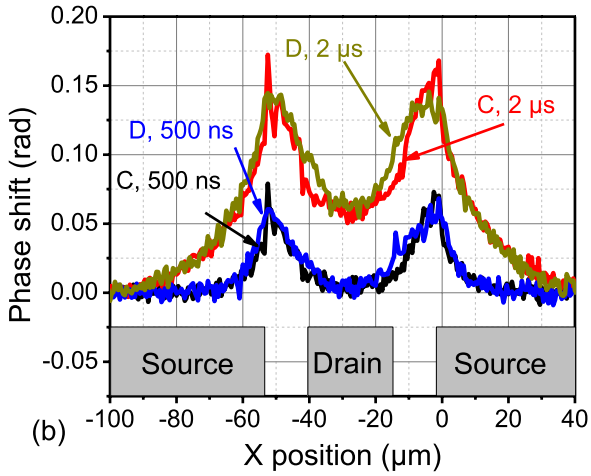

Fig. 6. TIM signals at 500 ns and 2 μs from the beginning of pulses for structures (a) A and B and (b) C and D.

Thus, for the short pulses, the heat spreading (both vertical and lateral) is not affected by Ar implantation in SiC alone (see comparison of TIM signals between structures C and D). Rather, higher Al content in the AlGaN buffer for structure B grown on Ar-implanted SiC can be assumed. Our finding

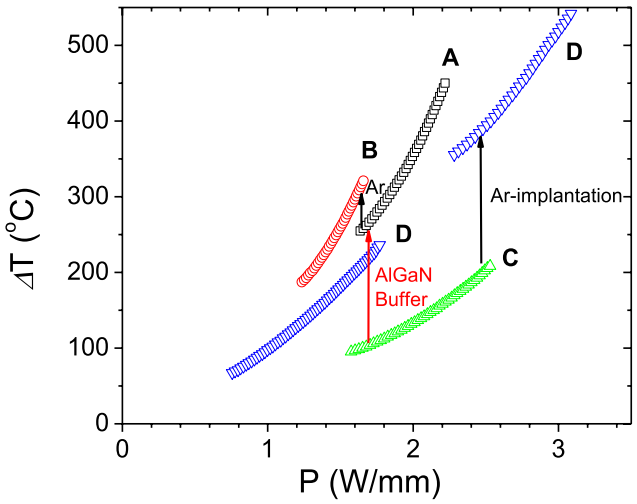

Fig. 7. DC temperature rises as a function of dissipated power for structures A–D. Arrows highlight the changes introduced to self-heating by different technological designs. For structure D, temperature rises measured both at $V_{GS} = 3$ V and $V_{GS} = 2$ V are shown.

also correlates with the reported intact structural quality of the buffer layer grown on Ar-implanted SiC [3], i.e., TIM difference between structures A and B may not be explained by degraded buffer. We speculate that changed properties of Ar-implanted SiC surface give different incorporation of Al during the growth and consequently increased Al mass fraction in the buffer. We note that even a slight variation in Al fraction between 0% and 10% may have a significant impact on K_{AlGaN} [14]. It was analyzed elsewhere that a small portion of alien atoms in host material produces profound effect on the phonon scattering [14]. Therefore, the thermal conductivity of the buffer of the structure B is minimal from all the studied samples with the most pronounced self-heating effect.

C. DC Self-Heating

In Fig. 7, we show extracted T values in the dc regime of devices as a function of dissipated power. Calculations were done using (1) for devices biased at $V_{GS} = 3$ V and $V_{GS} = 2$ V (structure D only) and by extrapolating $\Delta R_S = f(T)$ polynomial fitting curves. We note that ΔR_S thermal calibration was done only up to 180 °C, and thus temperature extraction above this limit is an estimate. Nevertheless, similarly as observed in transient measurements in Fig. 4, the level of the self-heating is dominantly controlled by the buffer composition. Thus, the highest device thermal resistance is observed for structures A and B and statement 1) from the previous paragraph can also be adopted for the dc regime. On the other hand, the dc regime brings qualitative differences in a role of Ar implantation as the heat in the dc case is removed also through the substrate. As shown in Fig. 6, the impact of Ar implantation can be partially screened in the devices with the low thermal conductance of the AlGaN buffer; however, it is clearly visible from the comparison between structures C and D having GaN buffer with the high thermal conductivity. Therefore, 3) device cooling in the dc state is partially blocked by the degraded lattice of Ar-implanted SiC.

IV. Conclusion

In conclusion, we studied pulsed and dc regime self-heating effects in GaN transistors designed for high-power operation using electrical and optical methods and by thermal simulation. It is found that replacing the GaN buffer with AlGaN significantly increases transistor's self-heating. On the other hand, Ar implantation to the SiC substrate does not play a role in shortly pulsed transistors with GaN buffer because of the heat confinement in the buffer, while it overall limits the device cooling in the dc state. Our findings point on possible tradeoffs that must be given in to consideration by designing high-power GaN transistors.

References

[1] J. Das *et al.*, "A 96% efficient high-frequency DC-DC converter using E-mode GaN DHFETs on Si," *IEEE Electron Device Lett.*, vol. 32, no. 10, pp. 1370–1373, Oct. 2011.

[2] J. Würfl *et al.*, "Techniques towards GaN power transistors with improved high voltage dynamic switching properties," in *Proc. IEEE Int. Electron Device Meeting*, Dec. 2013, pp. 6.1.1–6.1.4.

[3] P. Kotara *et al.*, "Vertical blocking voltage improvement of GaN HEMT structures on n-SiC by pre-epitaxial substrate implantation," *ECS J. Solid State Sci. Technol.*, vol. 2, no. 8, pp. N3064–N3067, 2013.

[4] O. Hilt, P. Kotara, F. Brunner, A. Knauer, R. Zhytnytska, and J. Würfl, "Improved vertical isolation for normally-off high voltage GaN-HFETs on n-SiC substrates," *IEEE Trans. Electron Devices*, vol. 60, no. 10, pp. 3084–3090, Oct. 2013.

[5] W. S. Tan, M. J. Uren, P. W. Fry, P. A. Houston, R. S. Balmer, and T. Martin, "High temperature performance of AlGaN/GaN HEMTs on Si substrate," *Solid-State Electron.*, vol. 50, pp. 511–513, 2006.

[6] S. Singhal *et al.*, "Reliability of large periphery GaN-on-Si HFETs," *Microelectron. Rel.*, vol. 46, no. 8, pp. 1247–1253, Aug. 2006.

[7] J. Kuzmik, P. Javorka, A. Alam, M. Marso, M. Heuken, and P. Kordoš, "Determination of channel temperature in AlGaN/GaN HEMTs grown on sapphire and silicon substrates using dc characterization method," *IEEE Trans. Electron Devices*, vol. 49, no. 8, pp. 1496–1498, Aug. 2002.

[8] J. Kuzmik *et al.*, "Transient thermal characterization of AlGaN/GaN HEMTs grown on silicon," *IEEE Trans. Electron Devices*, vol. 52, no. 8, pp. 1698–1705, Aug. 2005.

[9] J. Kuzmik, S. Bychikhin, D. Pogany, C. Gaquière, E. Pichonat, and E. Morvan, "Investigation of the thermal boundary resistance at the III-nitride/substrate interface using optical methods," *J. Appl. Phys.*, vol. 101, no. 5, pp. 054508-1–054508-6, Mar. 2007.

[10] O. Hilt, F. Brunner, E. Cho, A. Knauer, E. Bahat-Treidel, and J. Würfl, "Normally-off high-voltage p-GaN gate HFET with carbon-doped buffer," in *Proc. IEEE 23rd Int. Symp. Power Semicond. Devices ICs*, May 2011, pp. 239–242.

[11] J. Kuzmik *et al.*, "Buffer-related degradation aspects of single and double-heterostructure quantum well InAlN/GaN high-electron-mobility transistors," *Jpn. J. Appl. Phys.*, vol. 51, no. 5R, p. 054102, 2012.

[12] D. Pogany *et al.*, "Quantitative internal thermal energy mapping of semiconductor devices under short current stress using backside laser interferometry," *IEEE Trans. Electron Devices*, vol. 49, no. 11, pp. 2070–2078, Nov. 2002.

[13] *TCAD Sentaurus, User Manual, ver. G-2012.06*.

[14] W. Liu and A. A. Balandin, "Thermal conduction in $Al_xGa_{1-x}N$ alloys and thin films," *J. Appl. Phys.*, vol. 97, no. 7, pp. 073710-1–073710-6, Apr. 2005.

[15] A. Sarua *et al.*, "Thermal boundary resistance between GaN and substrate in AlGaN/GaN electronic devices," *IEEE Trans. Electron Devices*, vol. 54, no. 12, pp. 3152–3158, Dec. 2007.

[16] D. Brunner *et al.*, "Optical constants of epitaxial AlGaN films and their temperature dependence," *J. Appl. Phys.*, vol. 82, no. 10, pp. 5090–5096, Nov. 1997.

Ján Kuzmík received the Ph.D. degree from the Slovak Academy of Sciences, Bratislava, Slovakia, in 1991.

He was an Invited Professor with Hokkaido University, Sapporo, Japan, in 2012. Since 2013, he has been the Head of the Department of Materials and Electron Devices at the Institute of Electrical Engineering, Slovak Academy of Sciences, where he is focusing on III-N device physics, processing, and characterization.

Milan Ťapajna received the Ph.D. degree in electronics engineering from the Slovak University of Technology, Bratislava, Slovakia, in 2007.

He is currently a Senior Researcher with the Institute of Electrical Engineering, Slovak Academy of Sciences. His current research interests include the electrooptical characterization and reliability of microwave and switching GaN-based devices, in particular, MOS-HEMTs.

Lukas Válik, photograph and biography not available at the time of publication.

Marián Molnár received the M.Sc. degree in electrical engineering from the Slovak University of Technology, Bratislava, Slovakia, in 2010, where he is currently pursuing the Ph.D. degree with the Institute of Electronics and Photonics.

He joined the Advanced Materials and Device Analysis Group at the Institute for Microelectronics, Vienna University of Technology, Vienna, Austria, in 2012. He is currently a Researcher with the Institute of Electronics and Photonics.

Daniel Donoval, photograph and biography not available at the time of publication.

Clément Fleury received the Dipl.-Ing. degree in physics, electronics, and material engineering from the Grenoble Institute of Technology, Grenoble, France, and the Politecnico di Torino, Turin, Italy, in 2012. He is currently pursuing the Ph.D. degrree with the Vienna University of Technology, Vienna, Austria.

He has been involved in backside infrared device characterization with the Vienna University of Technology.

Dionyz Pogany received the Dipl.-Ing. degree in solid-state engineering from Slovak Technical University, Bratislava, Slovakia, in 1987, and the Ph.D. degree from the Institut National des Sciences Appliquées de Lyon, Villeurbanne, France, in 1994.

He has been with the Vienna University of Technology, Vienna, Austria, since 1995, where he has been an Associate Professor since 2003, involved in device characterization.

Gottfried Strasser received the Ph.D. degree in physics from the University of Innsbruck, Innsbruck, Austria, in 1991.

He became a Full Professor at the State University of New York, Buffalo, NY, USA, in 2007, and a Full Professor at the Vienna University of Technology (TU Vienna), Vienna, Austria, in 2009. He is currently the Head of the Center of Micro- and Nanostructures at TU Vienna.

Oliver Hilt received the Ph.D. degree in physics from the Free University of Berlin, Berlin, Germany, in 1995.

He joined sglux GmbH, Berlin, in 1999, where he was involved in developing a titanium dioxide-based widebandgap UV photodiode, where he was the CEO from 2003 to 2006. He joined the Ferdinand-Braun-Institut, Berlin, in 2006, where he is currently the Head of the GaN Power Electronics Group.

Frank Brunner, photograph and biography not available at the time of publication.

Joachim Würfl received the Ph.D. degree in electrical engineering from the Technical University of Darmstadt, Darmstadt, Germany, in 1989.

He joined the Ferdinand-Braun-Institut, Berlin, Germany, in 1992. In 2007, he was appointed as the Head of the newly implemented research area GaN electronics. In this function, he is managing several projects on GaN-based discrete power devices, X- and Ka-band MMICs, and high-voltage power devices.